

Early Detection of Fatigue Damage in Composite Materials

M. J. Salkind*

Sikorsky Aircraft, Stratford, Conn.

Early detection of fatigue damage in composite materials by nondestructive inspection (NDI) techniques has been demonstrated for $\pm 45^\circ$ glass/epoxy, $\pm 45^\circ/0^\circ$ graphite/glass/epoxy, and 0° graphite/epoxy. Modulus and temperature were monitored and a correlation between them observed. Axial modulus and torsional modulus changes differed and, as might be expected, were a function of the laminate orientation. Torsional modulus measurements and coin tap tests were performed at 0, 10^6 , 5×10^6 , and 10^7 cycles, on axial fatigue specimens. Three distinct regions were noted. In the primary region a small (2%) but rapid change in stiffness was noted in the first few thousand cycles. This was followed by a secondary region of little or no stiffness change. The tertiary region was characterized by an increasing rate of stiffness change leading to fracture. NDI procedures including holographic interferometry, ultrasonics, penetrant, and X-ray radiography were evaluated for fatigue damage detection. Combined torsional-bending fatigue tests were performed on 0° graphite/epoxy. Using a failure criterion of a percentage change of torsional stiffness, design curves for any combination of torsional and bending fatigue stress were constructed.

Introduction

ONE of the most challenging problems facing the designer of composite structures is that the failure mechanisms, criteria, and analyses developed for metals are not readily applicable to composites. Whereas metals exhibit one failure mechanism, cracking, composites exhibit many, including delamination, fiber-matrix debonding, fiber fracture, and matrix cracking. The designer can establish failure criteria for metal structures based on crack size which either approaches a critical length for fracture, or reduces the section sufficiently to make the structure stiffness critical. Detection is based on measuring the crack length. Composites, however, can begin to exhibit substantial changes in stiffness very early (less than 1%) in the total life to fracture. These stiffness changes are a consequence of the combined effect of the multiple failure mechanisms just described. In addition, because composite laminates are generally anisotropic and usually are loaded anisotropically, the stiffness changes are also anisotropic. This behavior has been reported for a wide variety of composite materials including glass, graphite, and boron reinforced epoxy, glass reinforced polyesters and polypropylene, and boron reinforced aluminum.¹⁻¹⁵

The challenge, then, is to relate quantitatively the changes in structural properties, stiffness, residual strength, and residual life, to the fatigue damage accumulating in the structure, and to develop techniques for detecting such damage nondestructively. Such techniques are necessary for in-service damage detection as well as for manufacturing quality con-

trol. Clearly, the change in stiffness which often accompanies fatigue damage can be used for in-service damage detection as well as for manufacturing defect detection. Another unique characteristic of composites is that they exhibit heat generation as a result of fatigue damage (Refs. 1, 4-8, 10, 11, 16) and temperature sensing can be used for in-service damage detection. In addition to stiffness and temperature monitoring, other means of nondestructive damage detection for composites include visual, coin tap, ultrasonic, radiography, holographic interferometry, and acoustic emission.¹⁷⁻³¹ The purpose of the current program was to evaluate these damage detection techniques for glass and glass/graphite-epoxy composite specimens undergoing laboratory fatigue testing.

Experiments

This paper encompasses observations made during two experimental programs. The first¹³ involved axial fatigue testing of a 1.5-in.-diam tubular specimen as seen in Fig. 1. The two laminate systems evaluated were a four-ply glass-epoxy ($\pm 45^\circ$)_S and a six-ply 0° glass and 45° graphite-epoxy ($\pm 45^\circ/0^\circ/\pm 45^\circ/0^\circ$)_T. Fatigue testing was conducted on a

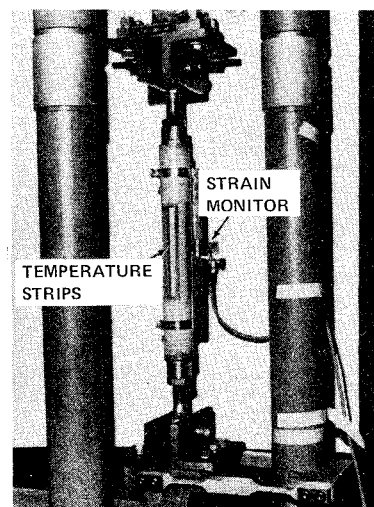


Fig 1 Axial fatigue test of tubular composite specimens.

Received May 16, 1975; presented as Paper 75-772 at the AIAA/ASME/SAE 16th Structures, Structural Dynamics, and Materials Conference, Denver, Colo., May 27-29, 1975; revision received April 5, 1976. This investigation was sponsored by the Air Force Office of Scientific Research under Contract F44620-73-C-0043 and is reported in AFOSR-TR-74-1791, Sept., 1974 and by the U.S. Army AMRDL-Langley Directorate and NASA under contract NAS1-12622 and is reported in NASA-CR-132414, Jan. 1974. The United States Government is authorized to reproduce and distribute reprints for governmental purposes notwithstanding any copyright notation hereon. The author would like to acknowledge gratefully the contributions of his coinvestigators, J. Lucas, J. Nevedunsky, and M. Ulichney.

Index categories: Aircraft Structural Materials; Reliability, Quality Control, and Maintainability; Structural Composite Materials (including Coatings).

*Chief, Structures and Materials. Presently Manager for Structures and Dynamics, NASA-Code RWS, Wash., D.C. Associate Fellow AIAA.

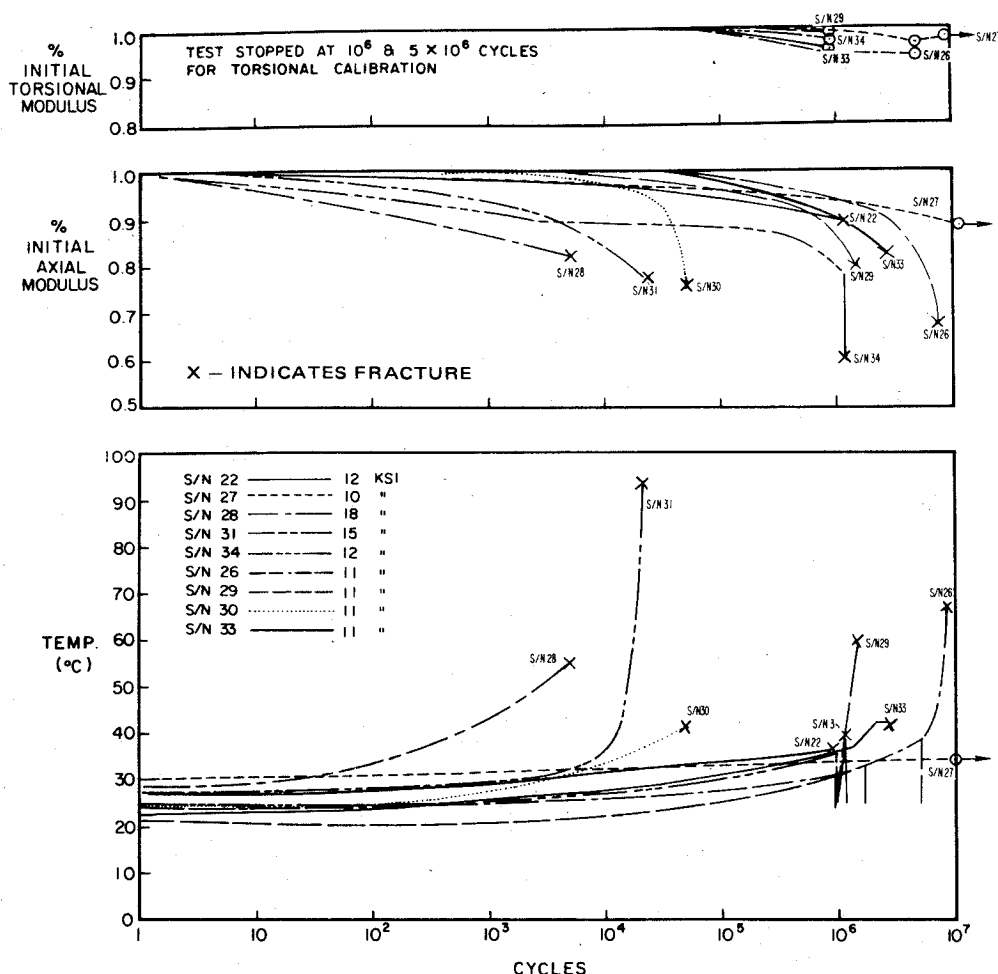


Fig. 2 Modulus reduction and corresponding temperature increase indicate irreversible fatigue damage and the onset of failure. ($\pm 45^\circ$)_S E-glass/epoxy specimens.

Sonntag SF-1-U constant load machine at a minimum-to-maximum stress ratio R of 0.1 (tension-tension) at 1800 cpm. Stiffness was monitored continuously using a mechanically attached displacement gage consisting of two strain gaged flexure arms (Fig. 1). Temperature was monitored continuously using thermocouples and temperature-sensitive paint strips and dots. At prescribed intervals, the tests were interrupted to conduct other examinations on the specimens, including torsional modulus testing, coin tapping, penetrant, ultrasonic, x-ray, and holographic interferometry.

The second program⁹ consisted of combined load fatigue testing of rectangular unidirectional graphite-epoxy specimens 1 in. wide, 0.1 in. thick, and having a 5-in.-long gage length (between doublers). Testing was accomplished using a specially built machine consisting of two bending eccentrics and one torsional eccentric to allow independent control of bending steady, bending vibratory, torsional steady, and torsional vibratory loads. Axial steady loads were controlled independently using springs, in series with the specimens, which do not restrict axial motion. The ratio of bending stresses in the thickness (flatwise) and width (edgewise) directions can be adjusted by rotating the specimen around its longitudinal axis so that the face and edge normals form the proper angle with the fixed bending vector. The grip attachment, consisting of a bolt circle, allows such adjustment.

Results and Discussion

Stiffness and temperature changes for the axially loaded tubular specimens are summarized in Figs. 2 and 3. The rate of temperature rise and modulus decrease changed concurrently during the fatigue tests as seen in Figs. 2 and 3. This

is evidence that both are indicating the same phenomenon, to wit, the rate of accumulation of fatigue damage. It should be noted that most fatigue specimens which fractured exhibited a rise in temperature just prior to fracture even when previously they had exhibited a leveling off of temperature. This observation is consistent with a more rapid accumulation of damage in the latter stages of fatigue. All of the specimens which were stopped at 10^7 cycles exhibited a leveling off of temperature. Had these tests been continued to fracture, it is believed that they too would exhibit a rise in temperature prior to fracture.

The damage detected in composites is also anisotropic in direction. The torsional modulus did not change to the same extent as the axial modulus. This phenomenon is thought to be related directly to the choice of specimen orientation and type of tests. Orientation of ($\pm 45^\circ$)_S and ($\pm 45^\circ/0^\circ/\pm 45^\circ/0^\circ$)_T would tend to sustain matrix damage while being tested in the axial direction. The axial modulus therefore would be expected to decrease. However, because the $\pm 45^\circ$ fibers still are continuous they still carry the load when loaded in torsion even though matrix damage exists. Thus, one would expect to observe less change in torsional stiffness. By contrast, 0° specimens would be expected to exhibit little change in axial stiffness but large changes in torsional stiffness,⁹ as discussed subsequently.

Three distinct regions were observed in the fatigue life of these materials. If one examines the initial stiffness behavior in an expanded scale (Fig. 4 shows the behavior of four typical samples), it is noted that there is a primary region of small stiffness change (2-5%) followed by a secondary region of little or no stiffness change. As seen in Figs. 2 and 3, the secondary region is followed by a tertiary region of in-

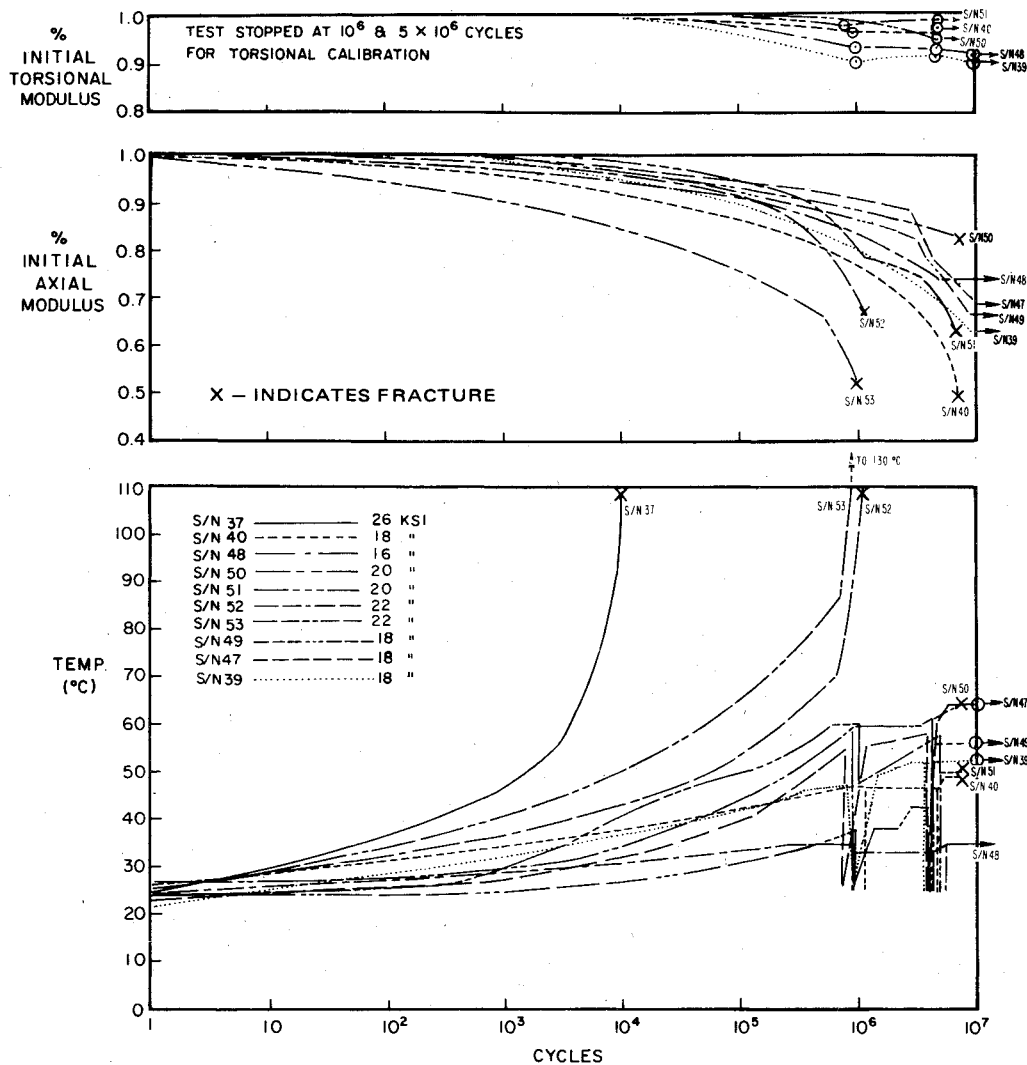


Fig. 3 Modulus reduction and corresponding temperature increase indicate irreversible fatigue damage and the onset of failure. $(\pm 45^\circ/0^\circ/\pm 45^\circ/0^\circ)_T$ graphite/glass/epoxy specimens.

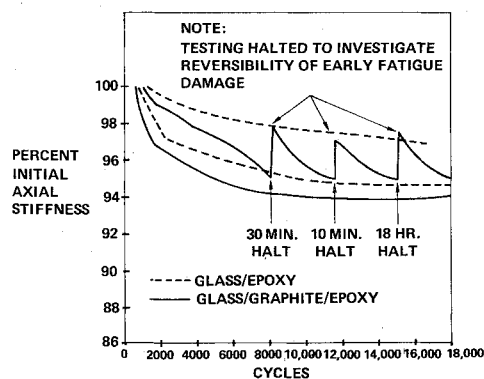


Fig. 4 Composites exhibit a primary stage of fatigue behavior in which a small change in stiffness occurs.

creasingly large stiffness change leading to fracture. The primary stiffness change is too small to note on the scale of Figs. 2 and 3. As seen in Fig. 4, one specimen was halted several times and cooled to ambient temperature in order to separate the stiffness change due to heating (about 2%) from that due to damage in the primary region (2-3%). The initial small stiffness change has been noted by several investigators^{12,15} and is probably because of failure of the weaker fibers and interfaces. Once these weak sources have

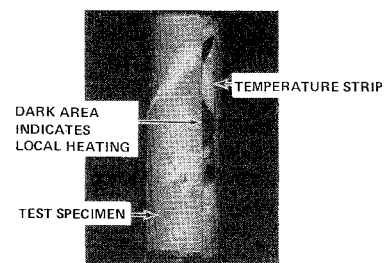


Fig. 5 Early local fatigue damage indicated by heating is detected by temperature sensitive strips.

been exhausted, the material enters the secondary stage during which little or no damage occurs. Significant fatigue damage accumulation results in the onset of the tertiary period.

Detecting local damage through local heating observations was accomplished by the use of temperature-sensitive coatings and strips. An example is shown in Fig. 5. It can be seen that local heating has turned regions of the white strip to black. This indicates that the temperature has exceeded 160°F locally. The specimen subsequently fractured along the line indicated by the heating.

Coin tap tests were conducted on all fatigue specimens. This procedure was found to be a poor indicator of early fatigue damage because significant indications were observed

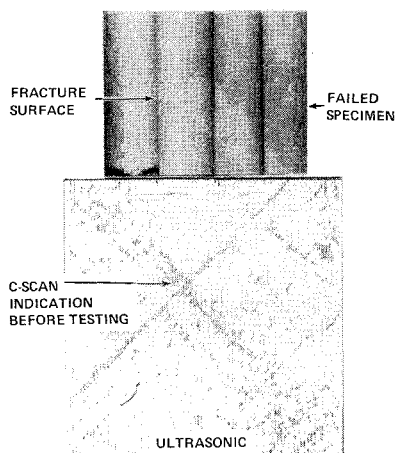


Fig. 6 Ultrasonic C-scan detected the presence of seam defects which ultimately resulted in fatigue fracture.

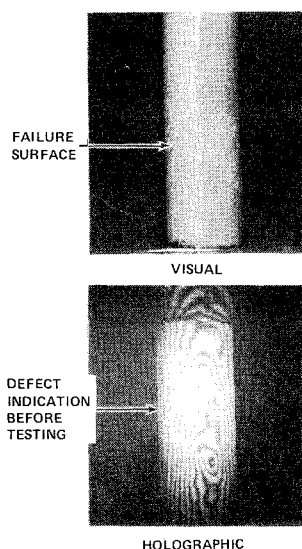


Fig. 7 Holographic inspection detected a defect in the composite tube, which ultimately resulted in fatigue fracture.

only at places of obvious visual damage. It is believed that the specimen configuration was too small to detect accurately any difference in pitch from one area to another because the sound was damped by the doubler and end plugs. Coin tap inspections might provide valid damage indication in large structures.

Specimens of each laminate chosen to undergo more substantial nondestructive evaluation were fatigue tested at a stress level designed to cause fracture between 5×10^6 and 10^7 cycles as determined from prior fatigue testing. At this level it was believed that sufficient fatigue damage would be present to evaluate the effectiveness of the nondestructive inspection methods. The damage detection methods employed were penetrant, ultrasonics, x-ray radiography, and holography and were performed at 0, 10^6 , 5×10^6 , and 10^7 cycles.

X-ray radiation was evaluated using "soft" x-rays of approximately 23 kV with a beryllium window but did not prove to be a valuable inspection technique. No void or crack indications appeared evident. Very faint indications of the specimen seams were visible. These seam indications can be detected more positively by ultrasonic inspection.

Ultrasonic inspection proved to be valuable in detecting the presence of defects at the seams of the $(\pm 45^\circ)_S$ glass/epoxy specimens, as shown in Fig. 6. A photograph of the fractured specimen also is shown in Fig. 6 and the fracture surface coincides with the locations of the indications in the ultrasonic C-

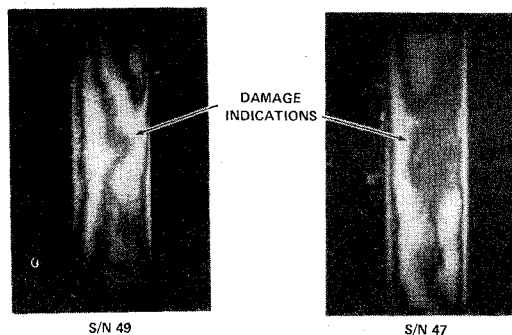


Fig. 8 Fatigue damage indications detected through holographic inspection.

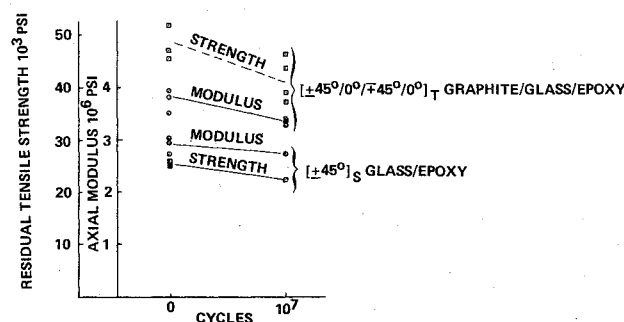


Fig. 9 Fatigue damage reduces axial residual strength and stiffness.

scan. Other than defects at the seams, no other indications of fatigue damage were noted in the glass specimens prior to fracture. By contrast, the graphite-glass specimens exhibited localized regions of fatigue damage which were detected after 10^7 cycles but not present at 5×10^6 cycles. Because these tests were terminated at 10^7 cycles, it is not clear whether or not these indications would have precipitated fatigue failure eventually. Additional work is needed in this area.

Holographic interferometry also was evaluated as a damage detection method. A defect detected in a glass/epoxy specimen by holography is seen in Fig. 7. Note that this coincides with the seam defect detected ultrasonically (Fig. 6). Defects also were detected in holograms taken at 10^7 cycles on graphite-glass specimens, as seen in Fig. 8. These indications of fatigue damage were not present at 5×10^6 cycles. The indications are also in approximately the same position as the damage indications present on the ultrasonic C-scan plots.

Specimens which did not fracture after 10^7 cycles were tested statically to failure to determine residual strength. These data are seen in Fig. 9 along with such data for unfatigued specimens and trend lines suggesting the rates of change. It should be noted that the structural damage indicated by stiffness change and temperature rise results in a significant reduction in the structural properties. These changes in stiffness and residual strength might constitute structural failure long before the structure is in danger of fracturing.

The results of combined load tests of uniaxial graphite epoxy are summarized in Table 1. The complexity of the test setup did not allow for continuous stiffness monitoring; however, the tests were stopped after 10^6 , 5×10^6 , and 10^7 cycles and both flexural and torsional (static) stiffness measured. It should be noted that these specimens exhibited significant changes in torsional stiffness and little change in flexural stiffness. This is because the damage is primarily in the matrix rather than the fiber dominated direction and is the exact opposite of the behavior of the $\pm 45^\circ$ laminates as noted earlier. If one selects a failure criterion of a 10% reduction in torsional stiffness, the data of Table 1 can be interpolated to yield the three design data points plotted in a combined load constant life design diagram as seen in Fig. 10. Adding the

Table 1 Test stresses and modulus reduction data

Specimen number	Steady axial, psi	Torsional stress, \pm psi	Flatwise bending, \pm psi	Edgewise bending, \pm psi	Initial static modulus, $\times 10^6$ PSI		Static modulus reduction at cycles, percent					
							10^6		5×10^6		10^7	
					Tors.	Flex.	Tors.	Flex.	Tors.	Flex.	Tors.	Flex.
04	4000	2420	37500	11600	0.78	14.20	4.7	2.0	10.8	2.6	10.8	5.7
06	4000	3300	51000	15100	0.78	13.33	8.2	2.5	11.9	2.7	12.0	5.0
08	4000	3850	59500	19200	0.74	13.30	5.1	0.0	9.6	1.2	43.8	6.5
03	4000	4850	25000	22300	0.72	12.99	18.5	4.0	30.7	17.6	70.0	19.3
09	8000	3510	15000	5380	0.72	13.70	5.8	0.5	7.8	1.0	7.4	0.5
05	8000	5610	20400	8080	0.74	13.36	7.2	1.0	5.6	1.9	5.9	2.9
07	8000	6540	23800	8540	0.73	14.06	7.4	1.5	38.5	3.4	56.2	3.9
01	8000	7480	27200	10900	0.72	13.56	8.5	3.1	29.7	4.1	73.6	5.1
11	12000	3510	15000	5330	0.78	12.72	3.0	0.0	0.0	2.9	3.5	2.6
10	12000	5610	20400	7750	0.72	13.72	9.2	0.0	11.5	2.5	12.6	3.0
02	12000	6540	23800	9050	0.75	13.52	12.8	2.4	39.5	3.3	45.2	2.4
12	12000	7480	27200	10300	0.73	13.28	13.3	0.4	17.3	0.4	50.0	0.4

same type of data from a pure torsion and a pure bending fatigue test yields a straight line relationship which can be used to describe the design limit for any combination of bending and torsion. There appears to be little sensitivity to the axial steady stress.

Conclusion

It appears that there are many indicators of early fatigue damage in composites which can be exploited to develop in-service detection schemes. Permanent changes in stiffness have been detected at less than 1% of total life to fracture.

Temperature monitoring, ultrasonics, and holography also have proved to detect damage at these early stages. Although each of these techniques is technically and economically feasible for in-service damage detection, their effectiveness depends to a large extent on defining a quantitative data base relating indications to residual strength and life. This research has laid the foundation for developing that data base, but extensive additional testing is needed. The behavior of different materials and laminate orientations should be defined in detail for all stages of fatigue life to provide a valid design data base.

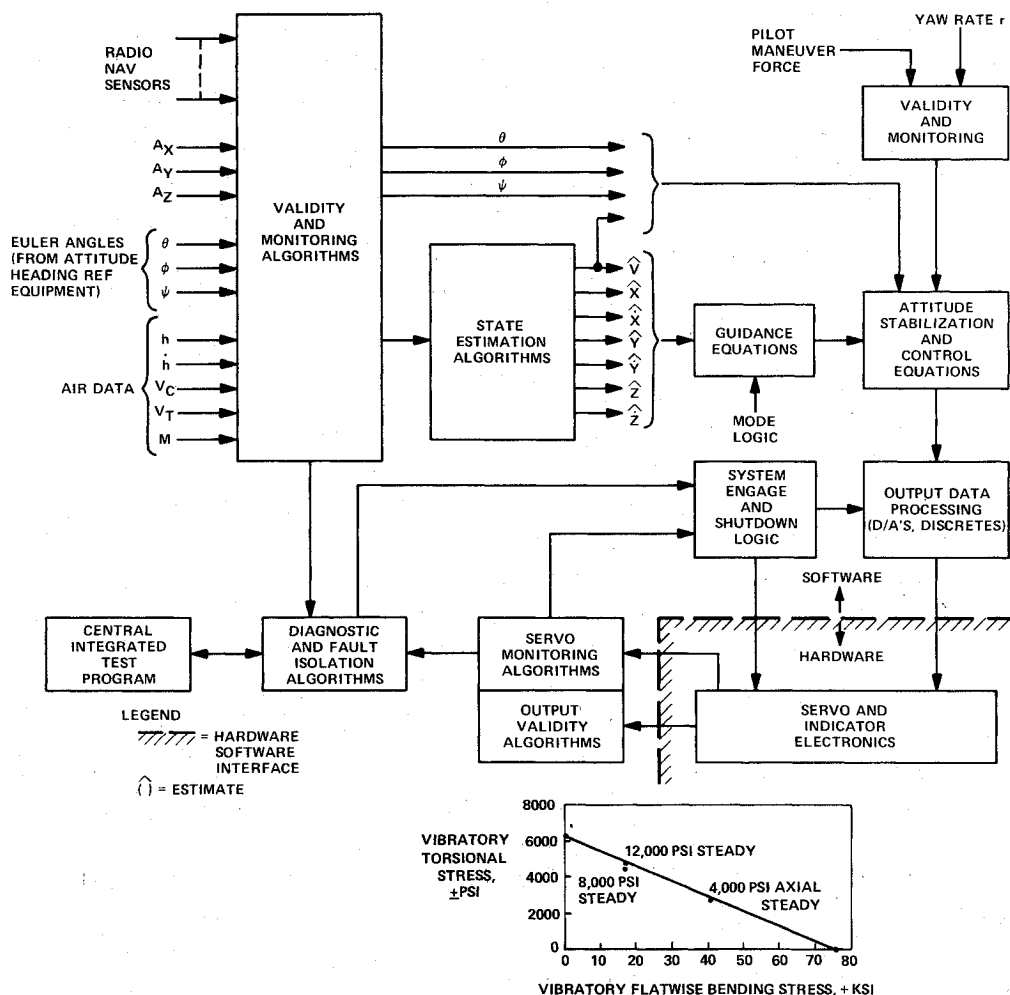


Fig. 10 Combined load fatigue diagram for graphite epoxy based on 10% torsional stiffness reduction at 10^7 cycles.

It should be noted that this type of research, which is material oriented, can provide only a part of the required design base for failsafe design of composite structures. There are other configuration-sensitive aspects which should be explored by complementary research efforts. These include such aspects as the fatigue behavior of bonded and mechanically fastened joints, the understanding of fatigue damage initiation and propagation, and the applicability of damage detection schemes to such joints.

References

- ¹Salkind, M. J., "Fatigue of Composites," *Composite Materials: Testing and Design (2nd Conference)*, STP497, 1972, American Society for Testing Materials, Phil., Pa., pp. 143-169.
- ²Broutman, L. J., Sahu, S., "Progressive Damage of Glass Reinforced Plastics During Fatigue," *Proceedings of 24th SPI Conference*, 11-D, Feb. 1969.
- ³Broutman, L. J. and Sahu, S., "A New Theory to Predict Cumulative Fatigue Damage in Fiberglass Reinforced Plastics," *Composite Materials: Testing and Design (2nd Conference)*, STP497, 1972, American Society for Testing Materials, Philadelphia, Pa., pp. 170-188.
- ⁴Reifsnider, K. L., Stinchcomb, W. W., Williams, R., and Marcus, L. A., "Heat Generation in Composite Materials During Fatigue Loading," AFOSR-TR-73-1961, May 1973, Virginia Polytechnic Institute.
- ⁵Cessna, L. C., Levens, J. A., and Thomson, J. B., "Flexural Fatigue of Glass Reinforced Thermoplastics," *Proceedings 24th SPI Conference*, 1-C, Feb. 1969.
- ⁶Reifsnider, K. L., Stinchcomb, W. W., Williams, R., and Turgay, H. M., "Frequency Effects on Composite Fatigue Reliability," STP580, 1975, American Society for Testing Materials, Phil., Pa.
- ⁷Stinchcomb, W. W., Reifsnider, K. L., Marcus, L. A., and Williams, R. S., "The Effects of Frequency on the Mechanical Response of Two Composite Materials to Fatigue Loads," *Fatigue of Composites*, STP569, 1975, pp. 115-129.
- ⁸Stinchcomb, W. W., Reifsnider, K. L., Marcus, L. A., Williams, R., "Effects of Cyclic Frequency on the Mechanical Properties of Composite Materials," AFOSR-TR-73-1907, July 1973, Virginia Polytechnic Institute.
- ⁹Ulitchny, M. G., and Lucas, J. J., "Evaluation of Graphite Composite Materials for Bearingless Helicopter Rotor Applications," NASA CR-132414, Jan. 1974.
- ¹⁰Boller, K. H., "Fatigue Fundamentals for Composite Materials," *Composite Materials: Testing and Design*, STP460, 1969, pp. 117-235.
- ¹¹Sturgeon, J. B., "Fatigue and Creep Testing of Unidirectional Carbon Fibre Reinforced Plastics," *Proceedings of 28th SPI Conference*, 12-b, Feb. 1973.
- ¹²Salkind, M. J., "Fiber Composite Structures," *Proceedings of the International Conference on Composite Materials*, AIME, N.Y., 1976, pp. 5-30.
- ¹³Nevedunsky, J. J., Lucas, J. J. and Salkind, M. J., "Fatigue Damage Behavior in Composite Materials," AFOSR-TR74-1791, Sept. 1974, Air Force Office of Scientific Research, Washington, D. C.
- ¹⁴Owen, J. J., "Fatigue Damage in Glass-Fiber-Reinforced Plastics," *Composite Materials, Vol. 5, Fracture and Fatigue*, Academic Press, N.Y., 1974, Chap. 7.
- ¹⁵Scott, D.H. and Gibson, J.S., "An Experimental Investigation of Stiffness Degradation in Graphite Composites," Rep. No. ER 10989, Dec. 1970, Lockheed, Georgia Co.
- ¹⁶Heller, R. A., Swift, G. N., Stinchcomb, W. W., Thacker, A. B., and Lui, J. C., "Time and Temperature Dependence of Boron Epoxy and Graphite-Epoxy Laminates AFML TR-73--261, Nov. 1973, Virginia Polytechnic Institute.
- ¹⁷Epstein, G., "Nondestructive Test Methods For Reinforced Plastic Composite Materials," Rept. No. SAMSO TR-69-78, Sept. 1972, Aerospace Corp.
- ¹⁸Martin, G. and Moore, J.F., "Research and Development on NDI Techniques For Composites," AFML - TR-68-202, June 1968, North American Rockwell.
- ¹⁹Zurbrick, J.R., "Development of Nondestructive Test Methods For the Quantitative Evaluation of Glass Reinforced Plastics," AFML-TR-66-269, March 1969, AVCO Corp.
- ²⁰Owston, C.N. and Jaffee, E.A., "Nondestructive Testing and Inspection Applied to Composite Materials and Structures," Rept. No. 590, 1971, AGARD, pp. 3-31.
- ²¹Rose, J.L., Carson, J.M., and Leidel, D.J., "Ultrasonic Procedures For Inspecting Composite Tubes," *Analysis of the Test Methods For High Modulus Fibers and Composites*, STP521, 1973, American Society for Testing Materials, Philadelphia, Pa., pp. 311-325.
- ²²Martin, G. and Moore, J.F., "Research and Development on NDT Techniques for Composites," AFML-TR-67-166, Nov. 1967, North American Aviation.
- ²³Martin, G. and Moore, J.F., "Research and Development on NDT Techniques For Composites," AFML-TR-67-166, Nov. 1967, North American Aviation.
- ²⁴Anderson, R.T. and DeLacy, T.J., "Nondestructive Testing of Composites," *Metal Progress*, Vol. 102, Aug., 1972, pp. 88-92.
- ²⁵Cook, J.L., Reinhardt, W.W., and Zimmer, J.E., "Development of NDT Techniques For Multidirectional Fiber Reinforced Resin Matrix Composites," McDonnell Douglas, AFML-TR-71-187, Oct. 1971, McDonnell Douglas.
- ²⁶Burchett, O.J. and Irwin, J.L., "Laser Holography of Carbon Composite Structures," *Carbon Composite Technology, Proceedings of the 10th Annual Conference*, 1970, American Society of Mechanical Engineers, p. 237.
- ²⁷McCaughy, W.A., Grant, R.M., and Brown, G.M., "Holographic Nondestructive Testing of Aircraft Materials," *Proceedings 15th National SAMPE Symposium and Exhibition*, Vol. 15, pp. 913-922.
- ²⁸Aas, H., Erf, R., and Waters, J., "Investigation to Determine the Feasibility of Employing Laser Beam Holography for the Detection and Characterization of Bond Defects in Composite Material Structures," Cr-111836, Feb. 1971, United Aircraft Research Labs, NASA.
- ²⁹Fitz-Randolph, J., Phillips, D.C., Beaumont, P.W.R., and Tetelman, A.S., "Acoustic Emission Studies of Boron-Epoxy Composites," *Journal of Composite Materials*, Vol. 5, Oct. 1971, pp. 542-548.
- ³⁰Williams, R.S. and Reifsnider, K.L., "Investigation of Acoustic Emission During Fatigue Loading of Composite Specimens," *Journal of Composite Materials*, Vol. 8, Oct. 1974, pp. 340-356.
- ³¹Lucian, A.D. and Standart, M.J., "The Application of Sonic and Microwave Inspections to Composite Nonmetallic Structures," *Proceedings of Aerospace-AFML Conference on NDT of Plastic Composite Structures*, March 1969, Dayton, Ohio.